

## Supporting information

### Carbohydrate Isomer Resolution *via* Multi-site Derivatization Cyclic Ion Mobility-Mass Spectrometry.

Kristin R. McKenna<sup>ab</sup>, Li Li<sup>abc</sup>, Andy Baker<sup>d</sup>, Jakub Ujma<sup>e</sup>, Ramanarayanan Krishnamurthy<sup>af</sup>, Charles L. Liotta<sup>ab</sup> and Facundo M. Fernández<sup>ab\*</sup>

<sup>a</sup>. NSF/NASA Center for Chemical Evolution

<sup>b</sup>. School of Chemistry and Biochemistry, Georgia Institute of Technology, Atlanta GA 30332, USA.

<sup>c</sup>. Current affiliation: Center for Alzheimer's and Neurodegenerative Diseases, Department of Biochemistry, University of Texas Southwestern Medical Center, Dallas, TX 75390, USA.

<sup>d</sup>. Waters Corporation, Pleasanton, CA 94588, USA.

<sup>e</sup>. Waters Corporation, Wimslow SK9 4AX, United Kingdom.

<sup>f</sup>. Department of Chemistry, The Scripps Research Institute, La Jolla, CA 92037, USA.

\*30332-0400. 901 Atlantic Dr. NW, Atlanta, GA, USA.

E-mail: facundo.fernandez@chemistry.gatech.edu; Fax: +1 (404) 894-7452;

Tel: +1 (404) 385-4432

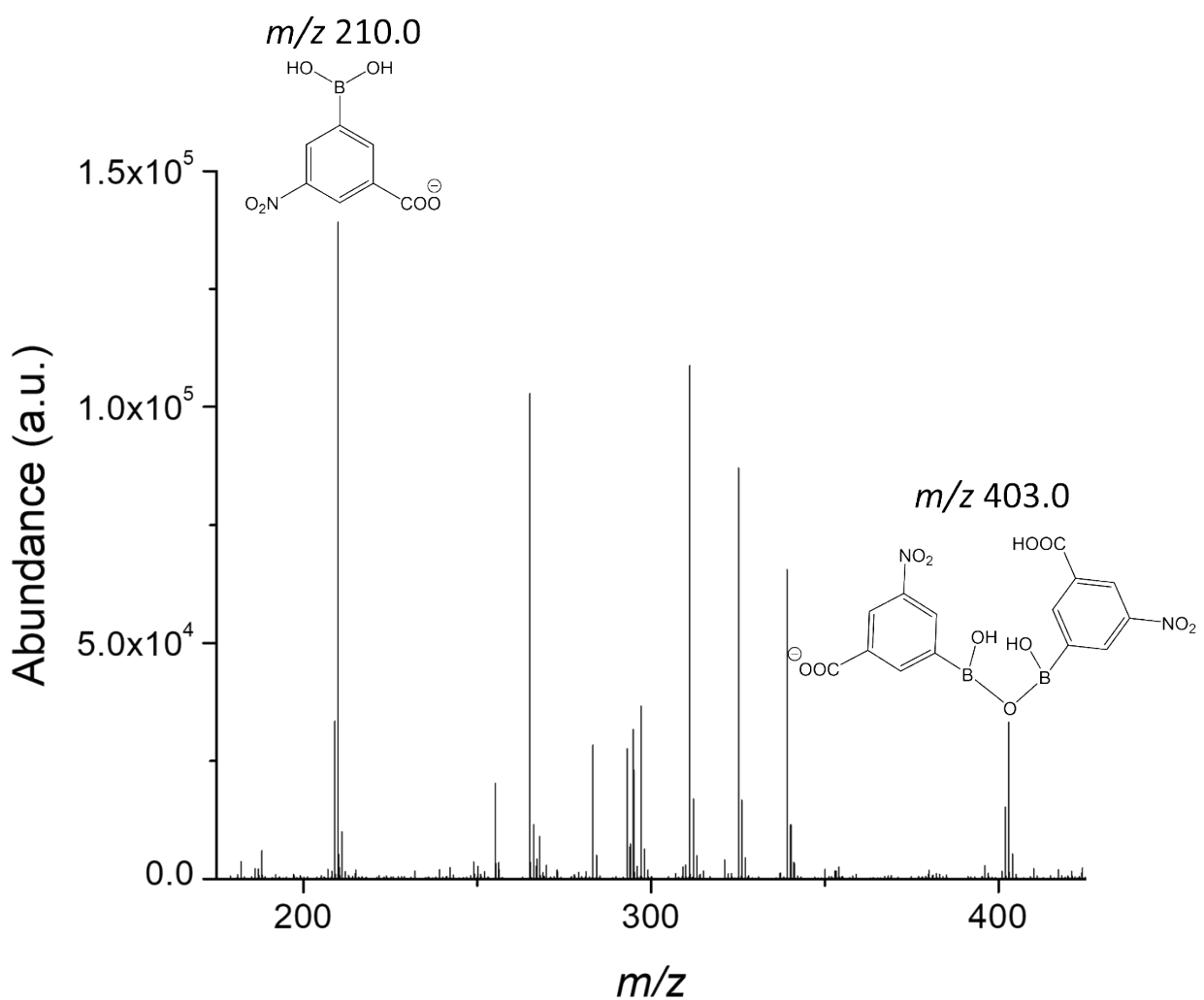


**Figure S-1.** Full scan MS data showing evidence for the presence of the anhydride dimer in the 3C5NBA reagent.

**Table S-1.** The number of possible regio- and functional isomers possible for each carbohydrate when reacting with two separate 3C5NBA molecules (left), the anhydride dimer of 3C5NBA (middle), and the total expected number of structures from the derivatization reaction for each carbohydrate (right). \* indicates that the sugar can undergo mutarotation, so more derivatives would be expected than for one stereoisomer.

Carbohydrate	# of Possible Boronic Acid Derivatives	# of Possible Dehydrated Anhydride Derivatives	Total Possible Derivatives
Fructose	1	1	2
Galactose	2	1	3
Glucose	1	2	3
Mannose	2	1	3
Cellobiose*	1	3	4
Isomaltose	1	4	5
Lactose*	2	2	4
Lactulose	4	1	5
Maltose	1	3	4
Melibiose	2	3	5
Sucrose	3	3	6
Trehalose	1	2	3

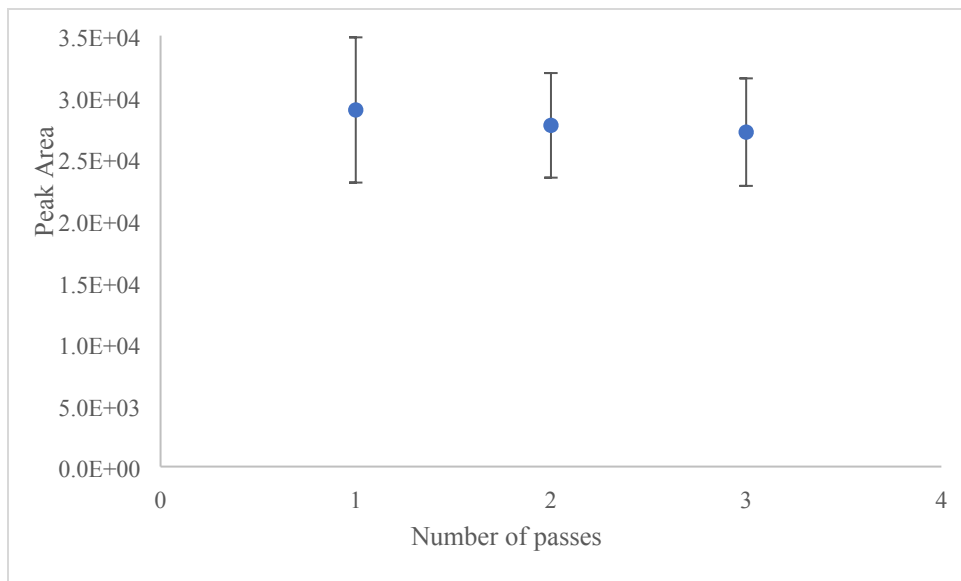


**Figure S-2.** Peak areas of the doubly derivatized glucose ( $m/z$  529) ion *vs.* the number of passes in the cyclic ion mobility device. Data points and error bars correspond to average and standard deviations from eight measurements, respectively.

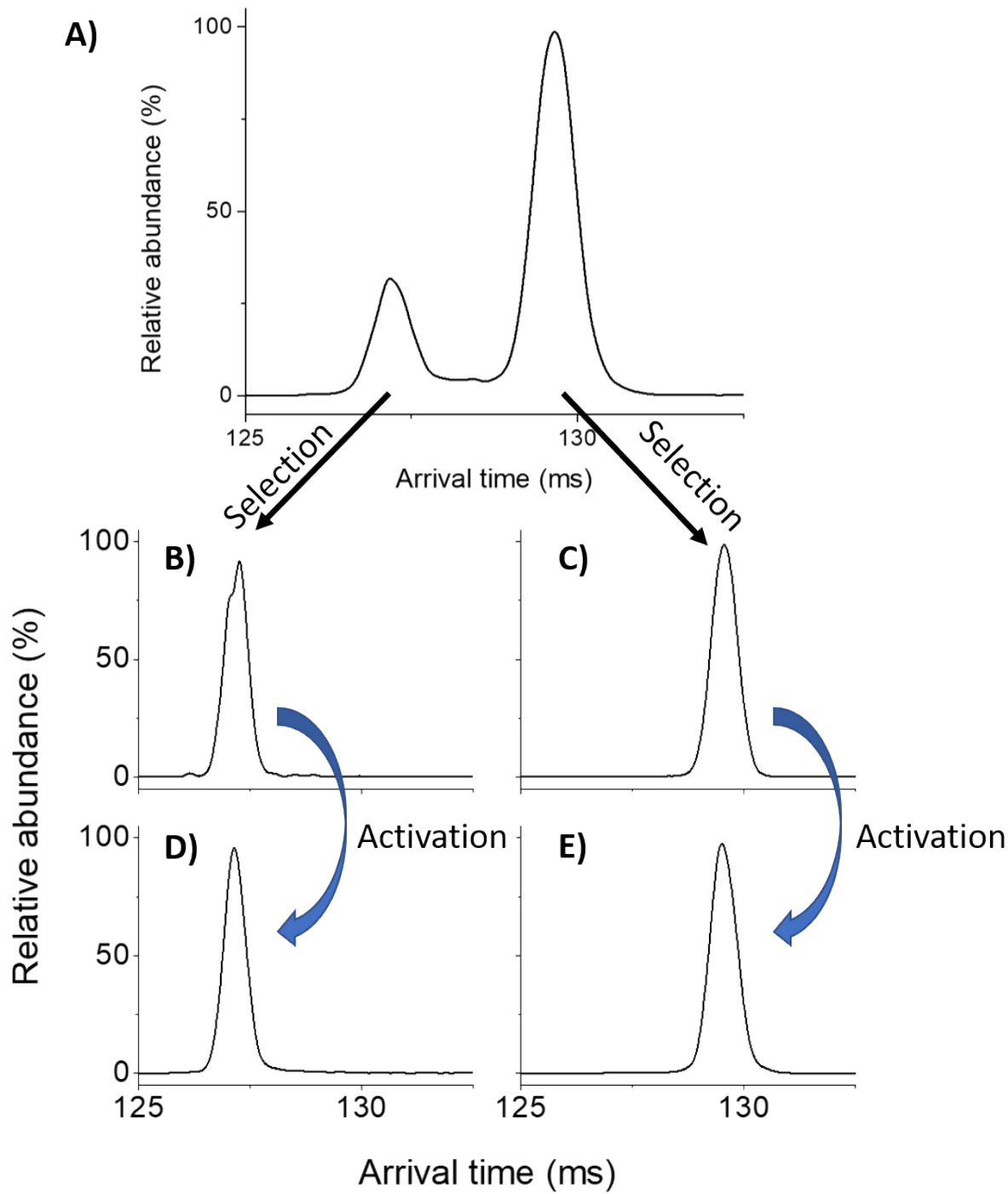


**Figure S-3.** (A) Arrival time distribution of doubly 3C5NBA-derivatized mannose after three cIM passes, followed by a frontflush of the mobility peaks with arrival times lower than 30 ms and an additional four passes. The selection of the mobility region containing each peak (injection into a pre-cIM store) after three cIM passes followed by an additional four passes after reinjection is shown in B) and C), with the results of the same method with the addition of activation during reinjection with a voltage offset (115 V) shown in D) and E). If there had been interconversion between these species, two peaks would have been observed in the ATD after activation.

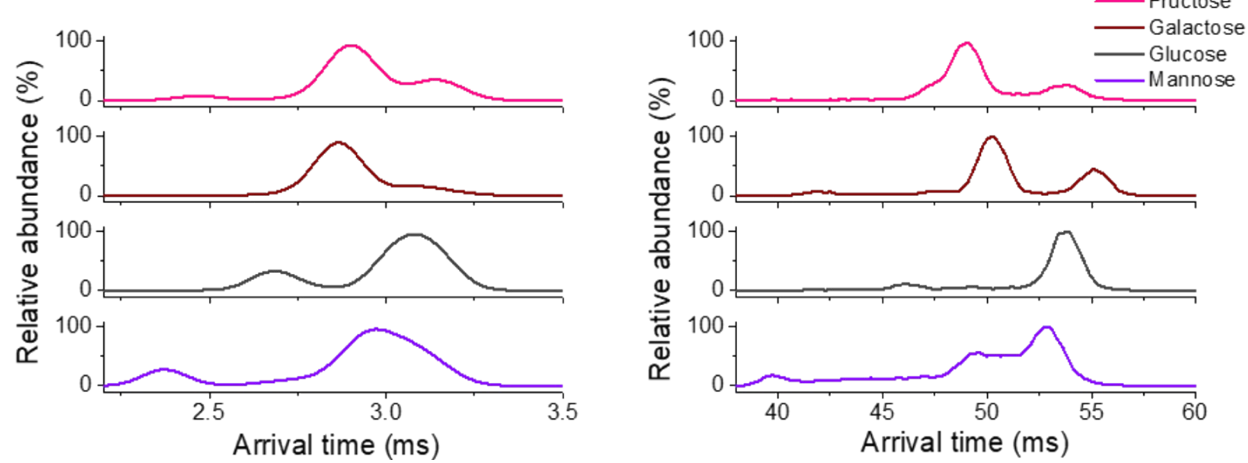


**Figure S-4.** Doubly 3C5NBA-derivatized monosaccharides analyzed on the Synapt G2-Si (left) and after three passes on the cIM instrument (right).

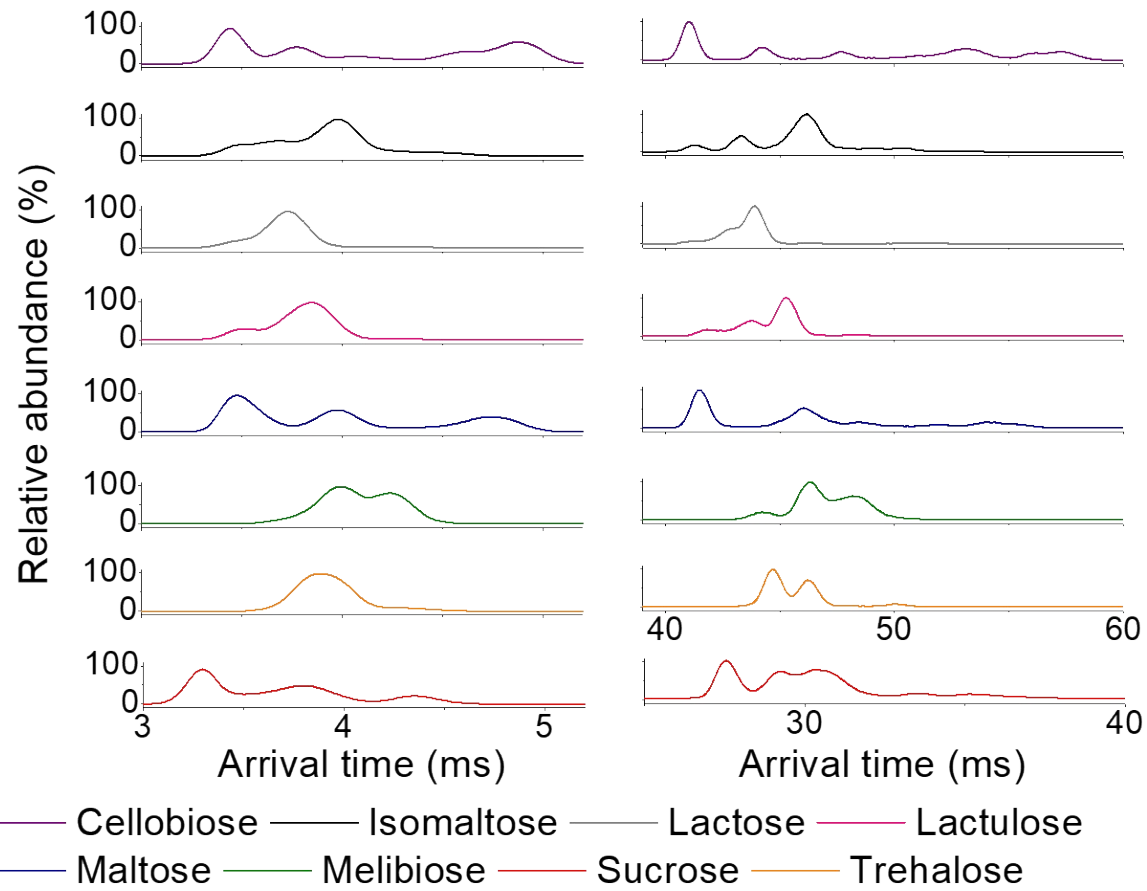


**Figure S-5.** Doubly 3C5NBA-derivatized disaccharides analyzed on a SYNAPT instrument (left) and the same analytes after three passes in the cyclic IM instrument (right). The right ATD for sucrose is shown after only two passes due to the observation of wraparound effects after three passes.

**Table S-2.** Two-peak resolution ( $R_{pp}$ ) of the most abundant monosaccharide 3C5NBA derivatives on the Synapt and the cIM systems after three passes.

Monosaccharide Pair	$R_{pp}$ (Synapt)	$R_{pp}$ (3 passes)
Fructose vs. Galactose	0.14	0.53
Fructose vs. Glucose	0.58	1.92
Fructose vs. Mannose	0.32	1.36
Galactose vs. Glucose	0.49	1.58
Galactose vs. Mannose	0.23	1.00
Glucose vs. Mannose	0.20	0.38

**Table S-3.** Two-peak resolution ( $R_{pp}$ ) of the most abundant disaccharide 3C5NBA derivatives on the Synapt and cIM systems after three passes.

Disaccharide Pair	$R_{pp}$ (Synapt)	$R_{pp}$ (3 passes)
Cellobiose vs. Isomaltose	1.57	3.37
Cellobiose vs. Lactose	0.87	1.44
Cellobiose vs. Lactulose	1.01	3.14
Cellobiose vs. Maltose	0.16	0.38
Cellobiose vs. Melibiose	1.09	1.55
Cellobiose vs. Sucrose	0.53	0.94
Cellobiose vs. Trehalose	1.12	2.89
Isomaltose vs. Lactose	0.63	0.99
Isomaltose vs. Lactulose	0.32	0.50
Isomaltose vs. Maltose	1.26	2.94
Isomaltose vs. Melibiose	0.07	0.07
Isomaltose vs. Sucrose	1.97	4.69
Isomaltose vs. Trehalose	0.13	0.88
Lactose vs. Lactulose	0.24	0.67
Lactose vs. Maltose	0.64	1.17
Lactose vs. Melibiose	0.50	0.60
Lactose vs. Sucrose	1.30	2.16
Lactose vs. Trehalose	0.39	0.42
Lactulose vs. Maltose	0.79	2.67
Lactulose vs. Melibiose	0.29	0.31
Lactulose vs. Sucrose	1.38	4.60
Lactulose vs. Trehalose	0.16	0.39
Maltose vs. Melibiose	0.92	1.38
Maltose vs. Sucrose	0.62	1.36
Maltose vs. Trehalose	0.91	2.41
Melibiose vs. Sucrose	1.36	1.93
Melibiose vs. Trehalose	0.15	0.47
Sucrose vs. Trehalose	1.45	4.40

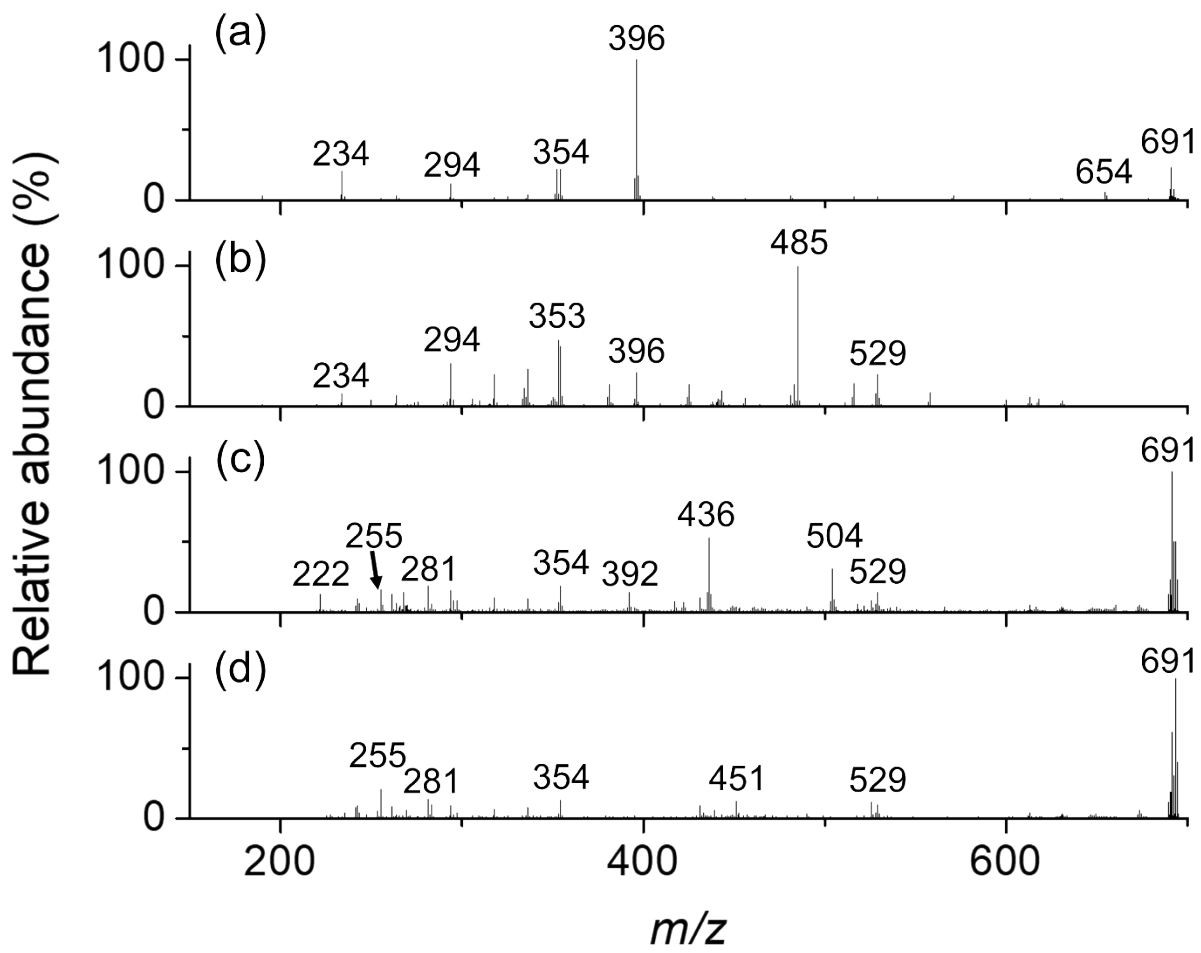


**Figure S-6.** Tandem MS spectra shown in a-d correspond to CID product ions generated from features I-IV in the maltose derivative ATDs in Figure 5.

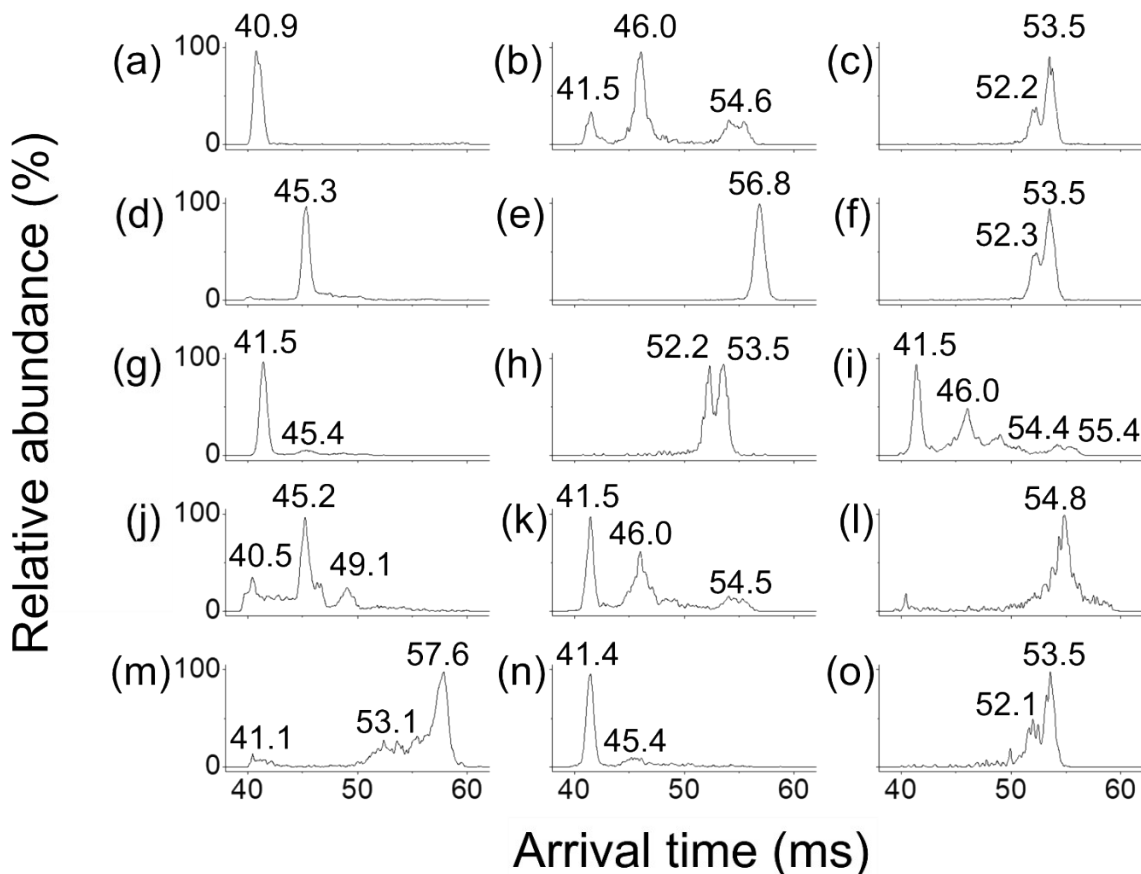


**Figure S-7.** ATDs for the doubly 3C5NBA-derivatized maltose precursor and MS/MS product ions at  $m/z$  (a) 654 ( $C_{26}H_{22}B_2N_2O_{17}$ ), (b) 529 ( $C_{20}H_{17}B_2N_2O_{14}$ ), (c) 504 ( $C_{18}H_{16}B_2N_2O_{14}$ ), (d) 485 ( $C_{18}H_{19}BNO_{14}$ ), (e) 451 ( $C_{18}H_{11}B_2N_2O_{11}$ ), (f) 436 ( $C_{17}H_8B_2N_2O_{11}$ ), (g) 396 ( $C_{15}H_{16}BNO_{11}$ ), (h) 392 ( $C_{16}H_{16}BNO_{10}$ ), (i) 354 ( $C_{13}H_{14}BNO_{10}$ ), (j) 353 ( $C_{13}H_{13}BNO_{10}$ ), (k) 294 ( $C_{11}H_{10}BNO_8$ ), (l) 281 ( $C_{14}H_9BNO_5$ ), (m) 255 ( $C_{12}H_7BNO_5$ ), (n) 234 ( $C_9H_6BNO_6$ ), and (o) 222 ( $C_8H_6BNO_6$ ). Certain fragments that correspond to the lowest abundance isomer III show some deviation in drift time, most likely due to low abundance and the overlap between III and IV convoluting the drift times.

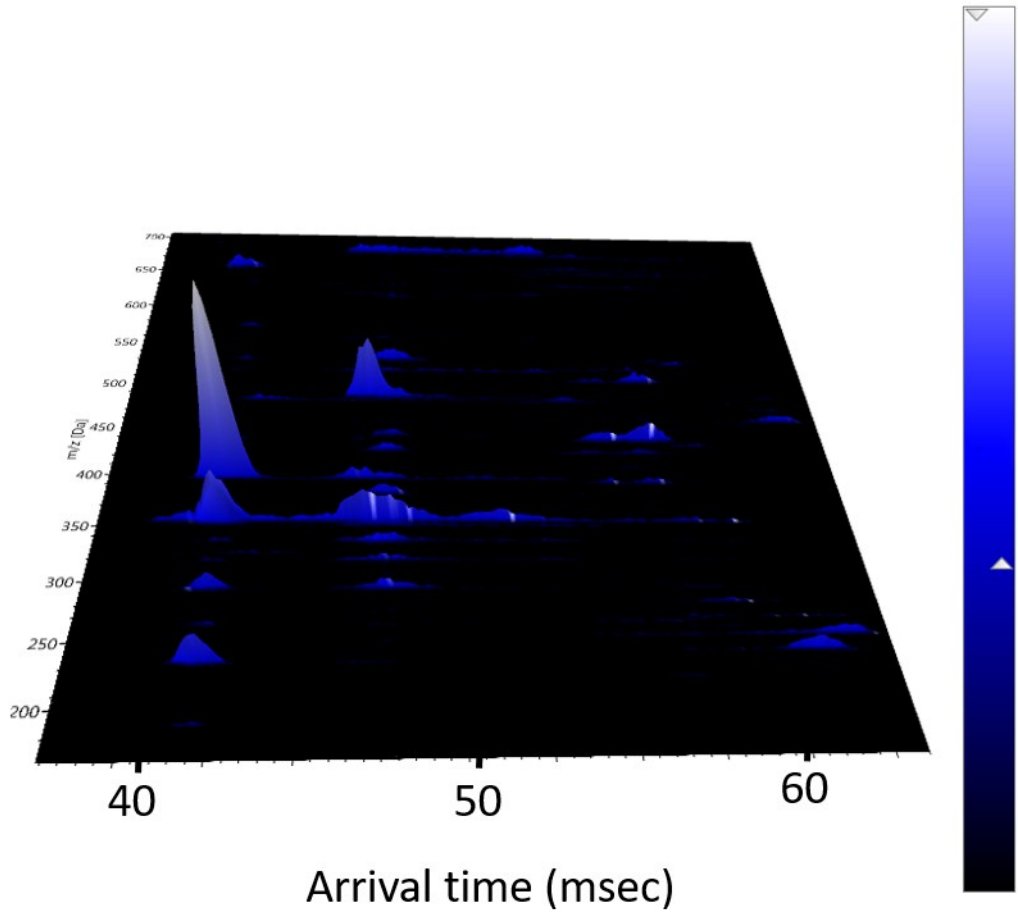


**Figure S-8.** A 2-dimensional plot showing the correlation between  $m/z$  and drift time of each of the doubly 3C5NBA-derivatized maltose MS/MS fragments.

**Table S-4.** MS/MS fragments observed for each monosaccharide derivative. Unique fragments are highlighted in yellow. Highlighted in blue are fragments that can distinguish isomers that have less than 1.00 resolution at three cIM passes without including isomers that are separated in the mobility dimension.

Fructose	Galactose	Glucose	Mannose
165.90	165.90	165.90	165.90
191.89	191.89	191.89	191.89
209.90	209.90	209.90	209.90
219.92	219.92	219.92	219.92
263.92	263.92	263.92	263.92
293.93	293.93	293.93	293.93
317.94	317.94	317.94	317.94
335.95	335.95	335.95	335.95
	353.97	353.97	
	384.94	384.94	384.94
	402.96	402.96	
438.97			438.97
441.02		441.02	
	468.99		
		511.01	511.01

**Table S-5.** MS/MS fragments listed for each disaccharide derivative. Unique fragments are highlighted in yellow.

Cellobiose	Isomaltose	Lactose	Lactulose	Maltose	Melibiose	Sucrose	Trehalose
		309.97	309.97	309.97			309.97
293.93	293.93	293.93	293.93	293.93	293.93	293.93	293.94
	275.92				275.92		
263.92	263.92	263.92	263.92	263.92	263.92	263.92	263.92
249.94	249.93	249.93	249.93		249.94	249.93	249.94
233.90	233.90	233.90	233.90	233.90	233.90	233.90	233.94
219.92	219.92	219.92	219.92	219.92	219.92	219.92	219.92
209.90	209.90	209.90	209.90	209.90	209.90	209.90	209.90
					194.89		
			191.8863		191.88		
189.91	189.90	189.91		189.91	189.91	189.90	189.90
165.89	165.91	165.91	165.91	165.88	165.90	165.89	165.90